Appl. Phys. B 32, 217–223 (1983)

Applied Physics B Photophysics and Laser Chemistry

Effects of "Atomic Depletion" on Four-Wave Mixing in Potassium

S. C. Mehendale, P. K. Gupta, and K. C. Rustagi

Laser Division, Bhabha Atomic Research Centre, Bombay-400 085, India

Received 27 June 1983/Accepted 1 August 1983

Abstract. Theoretical and experimental results are presented for a four-wave mixing process involving two photons generated internally by stimulated electronic Raman scattering. Effects of saturation of the Stokes wave due to loss of population in the ground state are analyzed in some detail. It is shown that phase mismatch and the absorption of the generated wave play an important role in determining the efficiency of the mixing process.

PACS: 42.65 Cq, 32.80 Kf

Four-wave mixing in atomic vapors has been investigated by several groups as a promising technique for optical frequency conversion [1–4]. Attractive features of atomic vapors in this regard are their large transparency ranges and the possibility of resonance enhancement of nonlinear susceptibility. Also, phase matching can be achieved by utilizing dispersion; modified, if necessary, by adding a suitable quantity of vapor of another metal. Of the various possible four-wave mixing processes, those which have one or more waves generated internally by stimulated electronic Raman scattering (SERS) merit special attention, since for these the nonlinear susceptibility can be quite large due to an exact two-photon resonance. A readily observable process of this type, which accompanies SERS, is generation of a down-converted beam at $\omega_4 = \omega_p - 2\omega_s$; ω_p and ω_s being the pump and the Stokes frequencies. This process was first observed by Sorokin et al. [2] in potassium vapor. In their experiment using a 1 kW dye laser, the four-wave output occurred over a relatively narrow range near the phase-matching point. With the use of high-power dye lasers the down-converted output has been observed over most of the spectral range in which SERS occurs [3, 5]. Corney and Gardner [6] presented a detailed experimental and theoretical investigation of the process in cesium vapor. Their theoretical analysis, assuming an exponentially growing Stokes wave, reveals the rather interesting feature that phase matching is unimportant so long as the phase mismatch Δk is smaller than the Stokes small-signal gain coefficient g_s. In fact, this applies equally to all four-wave mixing processes involving Stokes photons, as emphasized earlier by Kärkkäinen [4]. Recently, Heinrich and Behmenburg [7] have exploited this insensitivity to phase matching for tunable ultraviolet generation.

Theoretical treatments in [4 and 6] assume an exponential growth of the Stokes wave. Under typical experimental conditions, this is valid only near threshold, above which the Stokes output is saturated by atomic depletion [8–10] and pump depletion; the latter being important for large pump to Stokes conversion efficiency. In this paper, the process $\omega_4 = \omega_p - 2\omega_s$ is analyzed including saturation of the Stokes wave by atomic depletion. Our results clearly show that slower than exponential growth of the Stokes wave significantly affects the four-wave mixing process. Theoretical treatment in Sect. 1 shows that in the saturation region, the effect of phase mismatch becomes much more important than that predicted for exponential growth. Also the relative conversion efficiency to ω_4 can be much larger. Results of our experiments in potassium vapor are presented in Sect. 2. These are in good qualitative agreement with the theoretical findings. Section 3 presents our main conclusions.

1. Theoretical Analysis

Following Corney and Gardner [6], the growth of the electric field amplitude E_4 of the ω_4 wave is described

by

$$2k_4c^2\frac{\partial E_4(z)}{\partial z} = -\omega_4^2\chi^{(3)}(\omega_4)E_p(z)E_s^2(z)\exp(-i\Delta kz), \quad (1)$$

where E_p and E_s are the electric field amplitudes of the pump and the Stokes waves; other symbols have their usual meaning. Neglecting pump depletion and other saturation effects one has $E_p(z)=E_p$ and

$$E_s(z)=E_s(0)\exp(g_sz/2),$$

where

$$g_s=|\mathrm{Im}\{\chi^{(3)}(\omega_s)\}|\omega_s^2|E_p|^2/c^2k_s.$$

Substituting these into (1) it can be easily integrated to give for $g_sz\gg 1$ [Ref. 6, Eq. (9)]

$$I_4(z)=\frac{\omega_4^2}{4\omega_s^2}\left|\frac{\chi^{(3)}(\omega_4)}{\chi^{(3)}(\omega_s)}\right|^2\frac{I_s^2(z)}{I_p}\frac{1}{(1+\Delta k^2/g_s^2)}. \quad (2)$$

Thus, for $g_s\gg\Delta k$ the effect of phase mismatch is negligible.

However, since the assumption of exponential growth of the Stokes wave is not valid in almost all practical situations, applicability of (2) is limited. Cotter and Hanna [9] have shown that even when the conversion efficiency is low, the Stokes output is limited by atomic depletion over most of the tuning range. It may be noted that, in the small signal approximation most of the contribution to the Stokes output comes from a length $1/g_s$ at the end, hence atomic depletion may be important even when the total number of Stokes photons is much less than the total number of atoms in the path of the beam.

In the following we continue to neglect pump depletion, but consider the effect of atomic depletion. Then the Stokes wave first grows exponentially and then linearly in the saturation region. One model depicting this behaviour was described in [9]. For a rectangular pump pulse of duration τ, the Stokes energy per unit area is given by [Ref. 9, Eq. (10)]

$$\mathscr{E}_s(z)=\frac{Nhv_s}{2g_s}\ln\{1+\exp(g_sz)[\exp(\beta)-1]\},$$

where

$$\beta=2g_sn_s(0)c\tau/N.$$

N is the atomic density and $n_s(0)$ is the initial Stokes photon density.

As a simplification, we neglect temporal variation within the pulse and use an average Stokes intensity

$$I_s(z)=\mathscr{E}_s(z)/\tau$$
$$=[I_s(0)/\beta]\ln\{1+\exp(g_sz)[\exp(\beta)-1]\}, \quad (3)$$

where $I_s(0)=n_s(0)hv_s\,c$ is the Stokes noise tensity.

From [11], $n_{s0}=k_s\delta k_s/L$, δk_s being the Stokes line width and L the length of the vapor column. For typical experimental conditions, taking $N=5\times10^{16}\,\mathrm{cm}^{-3}$, $g_s=10\,\mathrm{cm}^{-1}$, $\tau=5$ ns, $L=20$ cm, and $\delta k_s=1\,\mathrm{cm}^{-1}$ gives $\beta\simeq10^{-11}$. Thus, (3) can be rewritten as

$$I_s(z)=[I_s(0)/\beta]\ln[1+\beta\exp(g_sz)]. \quad (4)$$

For small g_sz, the Stokes intensity grows exponentially from $I_s(0)$ while for large g_sz, such that $\beta\exp(g_sz)\gg1$, the growth is linear

$$I_s(z)=[I_s(0)/\beta](\ln\beta+g_sz). \quad (5)$$

In this model, departure from exponential growth occurs for $g_sz\sim|\ln\beta|$, which is nearly 25, for the value of β calculated above. This is comparable to the generally used threshold condition for observing SERS, viz $g_sz\simeq30$. It may be noted, however, that the use of a rectangular pump pulse overestimates Stokes energy and hence the saturation effects. For realistic smooth pulses saturation would occur for larger values of g_sz.

To consider the effect of saturation of the Stokes wave on the four-wave mixing process $I_s(z)$ given by (4) was substituted into (1). Since analytical solution is difficult, it was numerically integrated with values for various physical parameters given above. Figure 1 shows the variation of the intensity I_4, normalized to that for $\Delta k=0$, with phase mismatch Δk for different values of g_s. The dotted curve corresponds to the case of exponential growth described by (2). Thus, on including the saturation of the Stokes wave, I_4 falls much faster with increasing Δk. Also, in contrast to the prediction of (2), with larger g_s the effect of phase mismatch becomes more severe. This is physically understandable, since with larger g_s the region of saturated growth is increased. For $g_s=1$, the Stokes wave grows exponentially over the entire length, hence the two curves are identical. Another way to compare our results with the earlier theory is to calculate $I_4(z)$ corresponding to the same $I_s(z)$ in the two cases. Figure 2 shows the ratio I_4/I_4' as a function of g_s for different values of Δk, where I_4 is the intensity at ω_4 obtained by numerical integration and I_4' is the value calculated using (2), with I_s taken from (5). For $g_s\leqq1\,\mathrm{cm}^{-1}$ the two values are the same, while for $g_s>1\,\mathrm{cm}^{-1}$ the ratio increases rapidly. This implies that when the Stokes wave growth shows saturation behaviour, the relation between $I_4(z)$ and $I_s^2(z)$ can be different from that given by (2). In fact, the actual intensity can be much larger than that predicted by (2). With finite Δk, the ratio I_4/I_4' decreases compared to the $\Delta k=0$ value, although it can still be much greater than unity.

We have also considered the effect of linear absorption at ω_4 on the mixing process. Such absorption occurs

due to the presence of the alkali dimers. Figure 3 shows the intensity I_4 calculated for an absorption coefficient $\alpha=0.1$, expressed as a fraction of the corresponding intensity for $\alpha=0$, as a function of g_s. Initially, upto $g_s \sim 1.3$, the effect of absorption decreases with increasing g_s. In this region, the growth of the Stokes wave is nearly exponential, and then it can be easily shown that absorption reduces I_4 by a factor $g_s^2/(g_s+\alpha)^2$, which increases with g_s. For larger g_s, however, when saturation of the Stokes wave becomes important, the reduction in I_4 due to absorption is seen to increase with g_s. Thus, the effect of absorption is more important in the saturation region.

These effects of saturation of the Stokes wave on four-wave mixing, seen from the results of the numerical calculations can be understood more clearly by considering some limiting cases, which readily admit analytical solutions. For this, we note that approximation of the Stokes intensity by (5) is correct to within 5% for $z \geqq z_0$ where z_0 is given by $g_s z_0 = |\ln\beta| + 2$. For large g_s, z_0 is small, hence for sufficiently large z contribution to the four-wave mixing output from the initial length z_0 is small. Thus neglecting this as an approximation, E_4 can be obtained by integrating (1) from z_0 to z with the Stokes intensity given by (5). Defining $z'=z-z_0$, the length of the saturation region, for $\Delta k=0$ and $g_s z' > 1$, I_4 is found to be given by

$$I_4(z') = \frac{\omega_4^2}{16\omega_s^2}\left|\frac{\chi^{(3)}(\omega_4)}{\chi^{(3)}(\omega_s)}\right|^2 \frac{I_s^2(z')}{I_p} g_s^2 z'^2 . \tag{7}$$

Comparison with (2), which is valid for an exponentially growing Stokes wave, shows that in the saturation region the ratio I_4/I_s^2 can be much larger. This was seen in the results of the numerical calculations (Fig. 2), too.

For $\Delta k \neq 0$, retaining only the dominant terms the intensity at ω_4 has a growing part, proportional to z'^2 and an oscillating part varying like $\sin^2(\Delta k z'/2)$. The amplitude of oscillation becomes negligible compared to the growing term for sufficiently large z'. It may be noted, for comparison, that for an exponentially growing Stokes wave also, I_4 has an oscillating term varying like $\cos \Delta k z$. However, the ratio of amplitude of oscillation to the growing term is $2/\exp(g_s z)$ [Ref. 6, Eq. (8)], which is always vanishing small. Neglecting the oscillatory part, the ω_4 intensity in saturation region can be written as

$$I_4(z') = \frac{\omega_4^2}{4\omega_s^2}\left|\frac{\chi^{(3)}(\omega_4)}{\chi^{(3)}(\omega_s)}\right|^2 \frac{I_s^2(z')}{I_p} \frac{g_s^2}{\Delta k^2} .$$

Thus, the dependence on Δk is seen to be much stronger than that given by (2). Compared to the $\Delta k=0$ case, described by (7), the intensity at ω_4 is reduced by a factor $4/\Delta k^2 z'^2$. An interesting point to

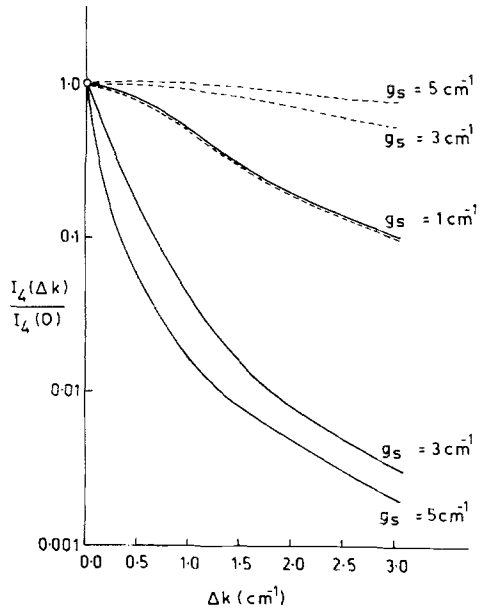

Fig. 1. Dependence of the ω_4 intensity at $Z=20$ cm on the phase mismatch Δk

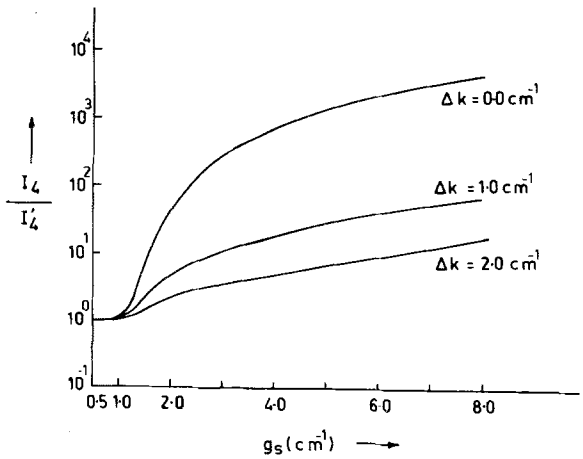

Fig. 2. Variation of the ratio I_4/I_4' defined in text, with the Stokes small-signal gain coefficient g_s, for different values of the phase-mismatch

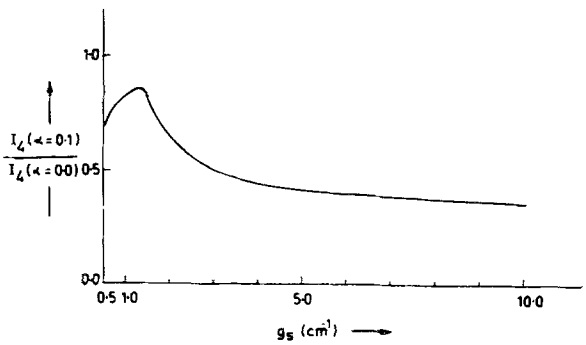

Fig. 3. Effect of absorption at ω_4 on the output intensity I_4 at $Z=20$ cm for different values of g_s

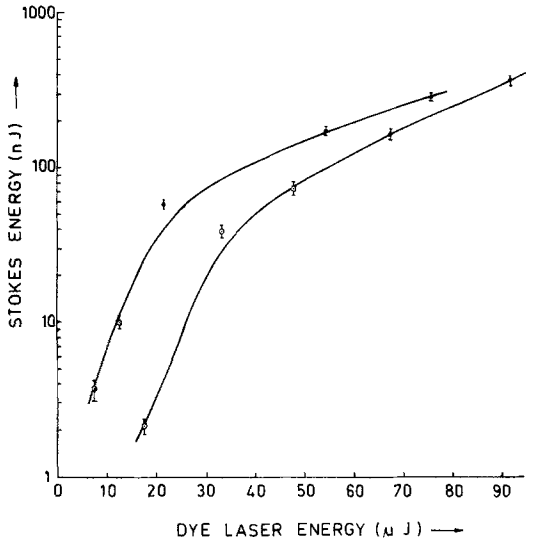

Fig. 4. Stokes output energy as a function of input dye-laser energy. The upper curve is for a vapor pressure of 5 Torr and the lower curve is for 1 Torr

note is that for $\Delta k \neq 0$, although for sufficiently large z', the four-wave output will not display Maker's fringes (since the oscillating part is negligible), the efficiency is, nevertheless, considerably reduced compared to the case of exact phase matching.

Thus it is clear that the saturation of the Stokes output alters the four-wave mixing process significantly. In this analysis, effects of spatial and temporal profiles and diffraction are not considered. Further, pump depletion is neglected which has to be included when the pump to Stokes conversion efficiency is large and also when the pump laser is tuned close to the resonance, when other loss mechanisms become strong. We have not included the change in $\chi^{(3)}(\omega_4)$ appearing in (1), due to the population transfer from the ground state, since the effect of this on the output at ω_4 is expected to be relatively small.

2. Experimental System and Results

Experiments were performed in potassium vapor using a nitrogen-laser pumped dye laser. The home-made nitrogen laser has an output power of 400 kW, a pulse duration of 10 ns and a repetition rate of 5 Hz. The dye-laser cavity was of the Hänsch design, with a 25 × telescopic beam expander and a 1800 lines/mm grating blazed at 4000 Å. A solution of di-phenyl stilbene in *p*-dioxane was used, which gave a tuning range of 396–416 nm. The dye-laser output power was 10–15 kW with a pulse duration (FWHM) of 6 ns and a spectral linewidth of about 1 cm^{-1}. The laser was not operating in the lowest transverse mode and the measured divergence was about 4 mrad.

Potassium vapor was generated in a stainless steel heat pipe oven heated to about 400 °C with argon as the buffer gas. The heated zone was 30 cm long. A quartz window was used at the input and a CaF_2 window at the exit to transmit the infra-red Stokes output. It was noted that the circulation of the metal was not adequate and a gradual accumulation occurred near the cold ends. After about twenty runs, it was necessary to push the metal towards the central region. Because of the uncertainty about the heat pipe action, the potassium vapor pressure was estimated from the external temperature of the oven, measured using a thermocouple.

The dye laser was tuned close to the $4s-5p$ resonance near 404 nm and focussed by a 30 cm focal length lens into the vapor column. The focal spot was estimated to be about 300 μm. The infra-red output was measured by a PbS detector which had a germanium window to cut off the dye laser and other visible emissions. The output at ω_4 was monitored by a photomultiplier tube (Philips 2232) placed at the exit of a 0.5 m monochromator. (Pacific Precision). The detectors gave information about the total pulse energy and were calibrated against a pyroelectric joulemeter (Molectron J3-05) with known calibration. The dye laser energy, the Stokes energy and the four-wave energy were measured successively, each for 10–20 shots. The fluctuations in the dye laser output were typically ±5%.

The down converted emission occurred over three wavelength ranges around 577,561 and 544 nm. These are identified as being due to the processes $\omega_p - 2\omega_{s1}$, $\omega_p - \omega_{s1} - \omega_{s2}$, and $\omega_p - 2\omega_{s2}$, respectively, where ω_{s1} and ω_{s2} correspond to the two Raman transitions $4s-5s$ and $4s-3d$. Although the two Stokes emissions were not separated in our infra-red measurements, the error introduced would be small, since the emission at ω_{s2} is known to be weak and occurs over a much narrower range [12]. In the following, detailed measurements for the process $\omega_p - 2\omega_{s1}$ are reported.

2.1. Saturation of the Stokes Output

Experimental observations of the saturation of the Stokes output by atom depletion have been reported by several groups [8–10]. Figure 4 shows the typical variation of the Stokes output energy with the dye laser energy under our experimental conditions. For the two curves, the pressures were about 1 Torr and 5 Torr and the dye laser frequencies were 24,734 and 24,811 cm^{-1}, respectively. The saturation is clearly seen. The maximum Stokes energy measured was 380 nJ, for a dye laser energy of 90 μJ, which corresponds to a photon conversion efficiency of 2.8%, thus the output was not limited by pump depletion. Another manifestation of the saturation was that the

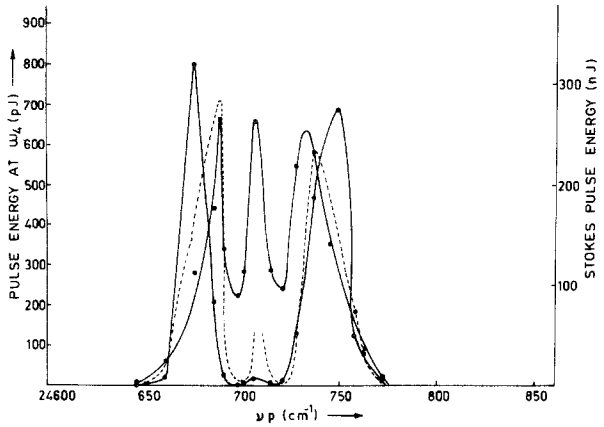

Fig. 5. Spectral tuning profiles for the stokes output (circled points ⊙) and the four-wave mixing output (filled circles ●) for vapor pressure of 1 Torr. Dotted curve is a suitably scaled, calculated tuning profile for output at ω_4. Near $\nu_p = 24{,}707\,\mathrm{cm}^{-1}$, the calculated energy at ν_4 becomes very large. This is shown by a break in the curve

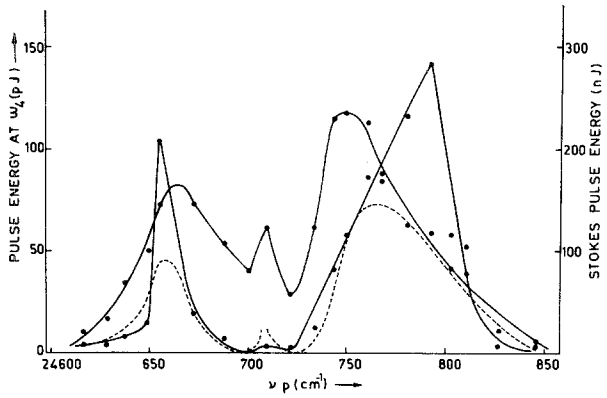

Fig. 6. Spectral tuning profiles, as in Fig. 5, for a vapor pressure of 5 Torr

fractional fluctuations in the Stokes output decreased with increasing dye laser energy, as was seen in [9] also.

2.2. *Spectral Dependence of the Output Energy at* ω_4

The measured Stokes and ω_4 output energies over the observed tuning range are shown in Figs. 5 and 6 for the two vapor pressures of 1 Torr and 5 Torr. The dashed curves give the suitably scaled energy at ω_4 calculated from the Stokes tuning profiles, using (2). The following features were noted in our results:

a) Except for the region between the two resonances at $24{,}701\,\mathrm{cm}^{-1}$ $(4s-5p_{1/2})$ and $24{,}720\,\mathrm{cm}^{-1}$ $(4s-5p_{3/2})$ the measured output energy at ω_4 was greater than the energy calculated from (2). For this calculation, the three waves were assumed to have similar pulse durations and spot sizes so that the intensities were replaced by energies in the equation and the measured value of the Stokes energy was used. The susceptibilities were calculated using the expressions given by Wynne and Sorokin [3] and matrix elements from Miles and Harris [13]. Maximum discrepancy occurred near the peak in the ω_4 output curve, on the high frequency side of the $4s-5p$ resonance, where the measured energy was larger by a factor of about 400 for the lower pressure and by about 10 for the higher pressure. The ratio decreased as ω_p changed on both sides of the peak and increased again for ω_p near the end of the Stokes tuning range and near the resonance, where the Stokes output was low. Similar behaviour was observed with ω_p tuned below the $4s-5p$ resonance also.

b) The observed four-wave output peaks were shifted from the positions of the calculated peaks so as to be away from the resonance. At the lower pressure, the shifts were 10–15 cm^{-1} for the two peaks in the curve for ω_4 one located below and one above the $4s-5p$ resonance. For the higher pressure, the calculated and observed peaks coincide on the low frequency side, while on the high frequency side the shift is larger, being about $30\,\mathrm{cm}^{-1}$. Within the resonance doublet, due to the moderate resolution of the monochromator used the number of points is too small to locate peak.

2.3. *Discussion of the Results*

a) The observed large departure between the calculated ($\mathscr{E}_4^{\mathrm{cal}}$) and the measured ($\mathscr{E}_4^{\mathrm{exp}}$) energies at ω_4 appears consistent with the results of the theoretical analysis in the preceeding section. There it was noted that under saturation conditions the ω_4 intensity can be much larger than that calculated from (2), which assumes exponential growth. In converting the equation from peak intensities to energies, which are experimentally measured, its right hand side has to be multiplied by a factor $\tau_p\tau_4/\tau_s^2 \times W_pW_4/W_s^2$ where the τ's and the W's are pulse durations and spot sizes. In the region of the saturated growth of the Stokes wave, the τ's and W's are expected to be of the same order for the three waves. Hence the observed departure seems to be due to non-validity of (2), rather than due to this factor. In the region of weak Stokes output, the growth of the Stokes wave would be nearly exponential and use of (2) should be justified. However, then $\tau_4 \sim \tau_s$, but $\tau_s \ll \tau_p$ and similarly for the spot sizes, making the multiplying factor large. The observed increase in the ratio $\mathscr{E}_4^{\mathrm{exp}}/\mathscr{E}_4^{\mathrm{cal}}$ in this region appears to be due to neglect of this factor in the calculation. This is also consistent with the measurements to be described in Sect. 2.4. With higher pressure the phase mismatch

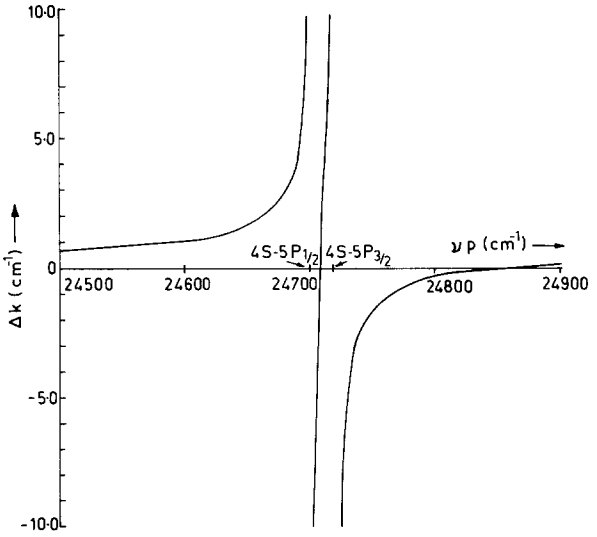

Fig. 7. Calculated phase-mismatch Δk as a function of the dye laser frequency

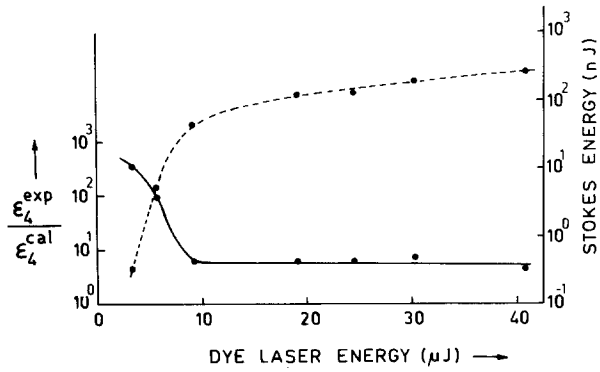

Fig. 8. Variation of the ratio of measured and calculated energies at ω_4 (continuous curve) and the corresponding stokes output energy (dashed curve) with the input dye-laser energy

Δk and the absorption at ω_4 would increase. Both these effects would contribute, in right direction to the observed decrease in the ratio at higher pressure.

The weak output within the resonance doublet is similar to the earlier observations by Sorokin et al. [2] and Kärkkäinen [4] on infra-red generation by difference frequency mixing in *K*. There this was attributed to the strong absorption of the pump beam and to other competing mechanisms, which become important due to the vicinity of the resonances. Another possible reason is the sharp variation of Δk in this region as shown in Fig. 7. Thus, depending on the exact dye laser frequency and bandwidth, the effective Δk can be large, which would reduce I_4. Also, since ω_p is in a strongly dispersive region effects like pulse broadening can occur. This region requires further investigation.

b) The effects of phase-mismatch are expected to become more important in the saturation region due to the $1/\Delta k^2$ dependence for I_4 predicted by (7). It is seen from Fig. 7 that $|\Delta k|$ decreases as ω_p is tuned away from the resonance, which can result in the observed shifts, Fig. 7 also shows that $|\Delta k|$ is asymmetric about the $4s-5p$ resonance especially for large detuning. On the low frequency side, it stabilizes to $\Delta k \simeq 1\,\mathrm{cm}^{-1}$, while on the high-frequency side, there is a phase matching point at $\omega_p = 24{,}860\,\mathrm{cm}^{-1}$. Since with increasing pressure, the Stokes peaks move away from the resonance, the observed asymmetry in the shifts at higher pressure can be due to the asymmetry in Δk. A similar shift between the peaks of the Stokes emission and the antistokes emission at ω_{as}, generated by a four-wave mixing process $\omega_{as} = 2\omega_p - \omega_s$, was observed by Takubo [10].

2.4. *Dependence of the Four-Wave Output on the Dye-Laser Energy*

Figure 8 shows typical variation of the ratio $\mathscr{E}_4^{\mathrm{exp}}/\mathscr{E}_4^{\mathrm{cal}}$, defined earlier, along with the corresponding Stokes energy with the dye-laser energy. For the dye-laser energy greater than 10 μJ, this ratio is nearly constant; while for lower energies it increases. This is contrary to the expectation that $\mathscr{E}_4^{\mathrm{exp}}/\mathscr{E}_4^{\mathrm{cal}}$ should decrease to unity near threshold since the growth of the Stokes wave would then be nearly exponential. This is believed to be a result of the differences in pulse durations and spot sizes, as mentioned in Sect. 2.3a. Experimental verification of this was, however, not possible due to the unavailability of a fast, sensitive detector.

3. Conclusions

To summarise, we have considered the effect of saturation of the Stokes wave due to atomic depletion on the four-wave mixing process $\omega_4 = \omega_p - 2\omega_s$. We have shown that in the saturation region, relative conversion to ω_4 can be more efficient and that the effects of phase mismatch and absorption at ω_4 become enhanced. Experimental results in potassium vapor are reported, which show significant departure from the earlier theory and which are in qualitative agreement with our theoretical predictions. Since atomic saturation of the Stokes wave is important in a wide range of experimental situations, the conclusions should be of relevence, also, to all four-wave mixing processes involving Stokes photons. When the Stokes output is limited by atomic saturation, minimizing phase mismatch, say by adding vapors of other atomic species should result in more efficient conversion.

Acknowledgements. It is a pleasure to thank Mr. S. Sasikumar for his able assistance throughout the course of this work. We are also grateful to Dr. D. D. Bhawalkar for valuable discussions and to Dr. R. Bhatnagar and Mrs. L. G. Nair for loan of equipment and experimental advice.

References

1. D.C. Hanna, M.A. Yuratich, D.Cotter: *Nonlinear Optics of Free Atoms and Molecules*, Springer Ser. Opt. Sci. **17** (Springer, Berlin, Heidelberg, New York 1979) pp. 251–270
2. P.P. Sorokin, J.J. Wynne, J.R. Lankard: Appl. Phys. Lett. **22**, 342–344 (1973)
3. J.J. Wynne, P.P. Sorokin: In *Nonlinear Infrared Generation*, ed. by Y.R. Shen, Topics Appl. Phys. **16** (Springer, Berlin, Heidelberg, New York 1977) pp. 159–213
4. P.A. Kärkkäinen: Appl. Phys. **13**, 159–163 (1977)
5. D. Cotter: Ph. D. Thesis (University of Southampton 1976) pp. 81–83
6. A. Corney, K. Gardner: J. Phys. B (Atom Molec. Phys.) **12**, 1425–1435 (1979)
7. J. Heinrich, W. Behmenburg: Appl. Phys. **23**, 333–339 (1980)
8. J.L. Carlsten, P.C. Dunn: Opt. Commun. **14**, 8–12 (1975)
9. D. Cotter, D.C. Hanna: IEEE J. QE-**14**, 184–191 (1978)
10. Y. Takubo: Appl. Phys. **24**, 139–142 (1981)
11. [Ref. 1, pp. 112–116]
12. P. Bernage, P. Niay, R. Houdart: Opt. Commun. **36**, 241–246 (1981)
13. R.B. Miles, S.E. Harris: IEEE J. QE-**9**, 470–484 (1973)

Responsible for Advertisements: E. Lückermann, G. Probst, Kurfürstendamm 237, D-1000 Berlin 15, Telephone: (0 30) 8 82 10 31, Telex 01-85411
Springer-Verlag Berlin — Heidelberg — New York. Printers: Brühlsche Universitätsdruckerei, Giessen, Printed in Germany